Digital microfluidics-enabled analysis of individual variation in liver cytochrome P450 activity

Gowtham Sathyanarayanan, Markus Haapala, Tiina Sikanen*

Faculty of Pharmacy, Drug Research Program, Division of Pharmaceutical Chemistry and Technology, Viikinkaari 5 E, 00014 University of Helsinki, Finland

*Correspondence to: tiina.sikanen@helsinki.fi, tel. +358-2941-59173

Abstract

The superfamily of hepatic cytochrome P450 (CYP) enzymes is responsible for the intrinsic clearance of the majority of therapeutic drugs in human. However, the kinetics of drug clearance via CYPs varies significantly among individuals due to both genetic and external factors, and the enzyme amount and function are also largely impacted by many liver diseases. In this study, we developed a new methodology, based on digital microfluidics (DMF), for rapid determination of individual alterations in CYP activity from human-derived liver samples in biopsy-scale. The assay employs human liver microsomes (HLMs), immobilized on magnetic beads to facilitate determination of the activity of microsomal CYP enzymes in a parallelized system at physiological temperature. The thermal control is achieved with the help of a custom-designed, inkjet-printed microheater array modularly integrated with the DMF platform. The CYP activities are determined with the help of pre-fluorescent, enzyme-selective model compounds by quantifying the respective fluorescent metabolites based on optical readout *in situ*. The selectivity and sensitivity of the assay was established for four different CYP model reactions, and the diagnostic concept was validated by determining the inter-individual variation in one of the four model reaction activities, i.e., ethoxyresorufin O-deethylation (CYP1A1/2), between five donors. Overall, the developed protocol consumes only about 15 µg microsomal protein per assay. It is thus technically adaptable to screening of individual differences in CYP enzyme function from biopsy-scale liver samples in an automated fashion, so as to support tailoring of medical therapies, for example, in the context of liver disease diagnosis.

1. INTRODUCTION

Precision medicine is an approach to patient care that aims to tailor medical therapies, i.e., select the most effective active pharmaceutical ingredient and adjust its dose in a personalized manner. One of the most critical biological processes impacting the blood concentration of drugs *in vivo* is the intrinsic metabolic clearance mediated by the hepatic cytochrome P450 (CYP) enzymes.[1,2] The CYP system is a superfamily of enzymes responsible for the elimination of the majority (70–80%) of clinical drugs, as well as many other xenobiotics. The metabolic capacity of CYPs, however, varies between individuals based on genetic variation (polymorphism) and many nongenetic factors such as diet, age, sex, and medication intake.[3] For example, the expression of CYP1A1 enzyme, which is responsible for the metabolism of many anti-cancer drugs as well as activation of procarcinogens, is largely impacted by several nongenetic factors.[4] Lifestyle choices, such as smoking, are known to affect the CYP1A1 expression levels and thus the hepatic clearance of anti-cancer drugs.[5] Also, environmental exposure to heavy metals increases CYP1A1 levels due to oxidative stress,[6] whereas exposure to pesticides inhibits its activity.[7] In addition, the CYP enzyme function is largely impacted by many liver diseases.[8,9] The inter-individual variation in drug clearance rate associated with CYPs is thus a major source of adverse drug effects and may lead to either toxic (slow metabolizers, too high blood concentration) or ineffective (rapid metabolizers, too low blood concentration) response. Although genetic CYP tests exist for distinguishing the rapid and slow metabolizer genotypes of certain polymorphic enzymes (e.g., CYP2C9 and CYP2D6),[10,11] these tests are not capable of predicting the inter-individual variation arising from external, nongenetic factors, or from progressive hepatic dysfunction associated with many severe diseases, including the COVID-19 pandemic.[12]

While the clinical utility of genetic CYP testing is debated, an alternative approach for direct measurement of the hepatic enzyme function is to dose patients with biomarkers (usually therapeutic drugs) that are known to selectively metabolize via certain CYP forms (e.g., caffeine demethylation via CYP1A2), followed by liquid chromatographic analysis of their plasma concentrations.[13] This, however, requires frequent blood sampling, possibly hospitalization, and is not necessarily feasible for critically ill and readily multidrug-treated patients. New diagnostic measures, such as biopsy-based testing, are therefore actively explored to account for individual variation in CYP-mediated

therapies and thereby support precision medicine strategies. To measure the hepatic CYP activities, microsomes are prepared from the tissue samples (typically collected from patients undergoing liver surgery) by differential centrifugation.[14,15] Human liver microsomes (HLM) are vesicle-like artifacts of the endoplasmic reticulum (ER) and enriched with microsomal CYPs, that reside on the cytosolic side of the ER.[16] HLMs (pooled from multiple organ donors) are currently routinely used the in the context of preclinical drug discovery, to examine the metabolic fate of new drug candidates *in vitro* and to predict the metabolic clearances *in vivo* with the help of appropriate scaling factors for microsomal protein content in the liver per body weight.[17,18] However, the information concerning individual variation in CYP activities is still rather limited owing to the scarce availability of tissue samples. It has been shown, nevertheless, that both the microsomal enzyme content and CYP activities vary significantly between patients[19–21], which stresses the need for new diagnostic measures that could foster the biopsy-scale analysis of CYP activities toward higher degree of automation and reduced sample consumption.

The recent progress in the development of digital microfluidics (DMF), a droplet manipulation technique based on electrowetting, has gained increasing attraction in point-of-care diagnostics and immunological assays.[22–24] In DMF, individual, tiny (typically nL–μL) sample droplets can be handled in parallel in an automated fashion, even by nonprofessional users. The robustness of the automated sample handling makes DMF a very promising technology for processing scarce patient samples in near-patient settings and clinical laboratories. A DMF-based assay is already been approved for clinical use in genetic disorder screening among newborns.[25] Likewise, the feasibility of DMF for the screening of patient-derived tissue (e.g., breast[26]) and liquid biopsies (e.g., dried blood spot[27]) has been demonstrated. However, the feasibility of DMF for CYP metabolism research has been only preliminarily shown by immobilizing human recombinant enzymes on porous polymer monolith plugs affixed onto the DMF platform, followed by fluorescence or ambient mass spectrometric detection of the produced metabolites.[28,29]

The aim of this study was to examine the feasibility of DMF for biopsy-scale analysis of CYP activities using human-derived liver samples. A quantitative DMF-based diagnostic assay was developed for manipulating HLM in droplets with a view to direct measurement of the hepatic CYP activity in a parallelized fashion *in situ*. This was accomplished by immobilizing HLMs on magnetic beads, which allows much better control over the total surface area compared with the previously employed porous polymer monoliths. The HLM-containing beads were then actuated by electrowetting and incubated with CYP enzyme specific model compounds at physiological

temperature achieved with modularly integrated, inkjet-printed microheater array. The technical feasibility of the assay for biopsy-scale analysis of hepatic CYP1A1/2 activity was demonstrated with five individual donor samples.

2. MATERIALS AND METHODS

Chemicals and reagents

The reagents used in the experiments included β-nicotinamide adenine dinucleotide 2′-phosphate reduced tetrasodium salt hydrate (NADPH), magnesium chloride, resorufin, acetone, methanol, ethylene glycol, acetonitrile, chloroform, dimethyl sulfoxide (DMSO), Trizma® base, 3-cyano-7-ethoxycoumarin (CEC), 3-cyanoumbelliferone (CHC), coumarin, umbelliferone, and fluorescein, all purchased from Sigma-Aldrich (Steinheim, Germany). Dibenzyl fluorescein was from Organix Inc. (Woburn, MA), 7-ethoxyresorufin from Toronto research chemicals (Toronto, ON), perchloric acid and potassium dihydrogen phosphate from Riedel-de Haën (Seelze, Germany) and dipotassium hydrogen phosphate from Amresco (Solon, OH). The lipids used for the preparation of fusogenic, biotinylated liposomes were from Avanti Polar Lipids, Inc. (Alabaster, AL) and included 1,2-dioleoyl-sn-glycero-3-phophoethanolamine (DOPE), 1,2-dioleoyl-3-trimethylammonium-propane chloride salt (DOTAP), 1,2-dioleoyl-sn-glycero-3-phophoethanolamine-N-(Cap biotinyl) sodium salt (biotin-cap-DOPE), and 1,2-dioleoylsn-glycero-3-phosphoethanolamine-N-(lissamine rhodamine B sulfonyl) (ammonium salt) (LissRhod B-DOPE). Water was purified with a Milli-Q water purification system (Merck Millipore, Molsheim, France).

Immobilization of human liver microsomes on magnetic beads

The method development was conducted with the help of commercially available human liver microsomes (HLM), pooled from 20 donors (#452161, Corning, Wiesbaden, Germany), and the method validation with the help of individual donor HLMs also available via Corning (#452138). For conducting the enzyme activity determination on DMF devices, the HLMs were immobilized onto streptavidin-coated magnetic beads (Dynabeads® M-280, Thermo Fisher Scientific, Vilnius, Lithuania). The Dynabead stock solution contains $6–7\times10^8$ beads (equivalent to 10 mg dry weight) per mL. Hereafter, a bead concentration of 6×10^8 beads per mL is used for all further calculations. Before immobilization, the HLMs were biotinylated with the help of fusogenic, biotin-containing liposomes following a previously reported protocol.[30] To prepare the liposomes, the DOPE, DOTAP, biotin-cap-DOPE, and LissRhod B-DOPE lipids were dissolved in chloroform and mixed in a weight ratio of 1:1:0.1:0.05, evaporated to dryness under nitrogen and kept under vacuum for 2 h prior to re-

solubilizing with PBS to a total lipid concentration of 2 mg/mL. To yield unilamellar fusogenic liposomes, the lipid mixture was extruded through a polycarbonate membrane (pore size = 100 nm, Avanti Polar Lipids, Alabaster, AL), and finally mixed and allowed to fuse (37 °C, 15 min) with the HLM (20 mg/mL total microsomal protein content) in a volumetric ratio of 1:1 to transfer the biotin-tag to the microsomal membrane. This yielded 10 mg/mL microsomal total protein concentration of biotinylated HLM (b-HLM).

Next, the b-HLM was applied on dry, streptavidin-coated Dynabeads and allowed to immobilize at room temperature for 30 min (on a rotating mixer). Before use, the magnetic Dynabeads were pretreated according to the supplier's protocol. In this study, 25 μL of b-HLM solution (i.e., 250 μg microsomal total protein) was used for functionalizing one batch of beads (0.25 mg dry weight, equivalent to 15 million beads). This protein amount (250 μg) was considered to represent the mean amount of microsomal total protein acquired from one liver biopsy: A typical biopsy mass is between 3–10 mg[19] (for calculation, a mean value of 6.5 mg was used) and the mean microsomal total protein of ca. 40 μg per mg liver (n=128 human liver samples) has been reported in the literature.[20] Thus, according to our protocol, 15 million magnetic beads were functionalized with microsomal protein amount equivalent to that derived from a liver biopsy. This amount of beads sufficed for ca. 15 on-chip enzyme incubations as explained later. After functionalization, the supernatant was discarded, the beads were washed three times with PBS, and finally, resuspended with PBS to yield final concentration of ca. 0.6 million beads/μL. Unless immediately used, the functionalized beads were refrigerated in PBS until use.

Digital microfluidic chip design and fabrication

The DMF chip design developed in this study included bottom (driving electrodes) and top (ground electrode) plates and an inkjet-printed four-in-one microheater (Fig 1 a–c). The bottom plate design consisted of an array of 72 driving electrodes, eight reservoir electrodes, and eight dispensing electrodes (Fig 1a). The DMF electrodes were patterned by photolithography onto a commercial glass substrate (Telic Company, Valencia, CA) pre-coated with chromium (100 nm) and AZ 1500 photoresist (530 nm). The electrodes were patterned by UV exposure (Dymax 5000-EC, Dymax Corporation, Torrington, CT; 5 s, nominal power 225 mW/cm^2) through a high-resolution plastic mask (Micro Lithography Services Ltd., Chelmsford, UK) and developed in AZ 351B developer (MicroChemicals GmbH, Ulm, Germany) for 20 s, followed by chromium etching in 3144 Puranal etchant (Honeywell International, Morris Plains, NJ) for 45 s, and resist removal in an acetone ultrasound bath for 10 min. In this work, a thiol-ene polymer was used as the dielectric layer to DMF.

The dielectric performance evaluation of thiol-ene polymer is reported in [31]. Before the dielectric coating, the contact pads on both sides of the bottom plate were covered with dicing tape. The thiol-ene pre-polymer was prepared from tetrafunctional 'thiol' (pentaerythritol tetrakis (3-mercaptopropionate), >95%, Bruno Bock Chemische Fabrik GmbH & Co. KG, Marschacht, Germany) and a trifunctional 'ene' (1,3,5-triallyl-1,3,5-triazine-2,4,6(1H,3H,5H)-trione, 98%, Sigma-Aldrich) mixed in a stoichiometric ratio, and incorporating 0.1% (*m/v*) Irgacure TPO-L as the photoinitiator (BASF, Ludwigshafen, Germany; 10%, *m/v*, in methanol). Next, the thiol-ene pre-polymer mixture was degassed under vacuum, spin-coated onto the electrodes at 2000 rpm for 30 s, and cured by UV flood exposure for 2 s (Dymax 5000-EC) (Fig 1d). Last, a fluoropolymer layer (1% FluoroPel PFC 1604V, Cytonix LLC, Beltsville, MD, diluted in Cytonix PFC 110 fluoro-solvent) was spin-coated onto the thiol-ene layer at 1200 rpm for 30 s, and the substrate was baked at 150 °C for 30 min (Fig 1d). The DMF top plate was a commercial indium tin oxide coated glass plate (Structure Probe Inc., West Chester, PA), which was coated in-house with fluoropolymer by the same process as the bottom plate. The top and bottom plates were then assembled, as shown in Fig 1a, with two layers of double-sided Scotch® tape (3M Company, Maplewood, MN) to achieve spacing of ca. 180 µm.
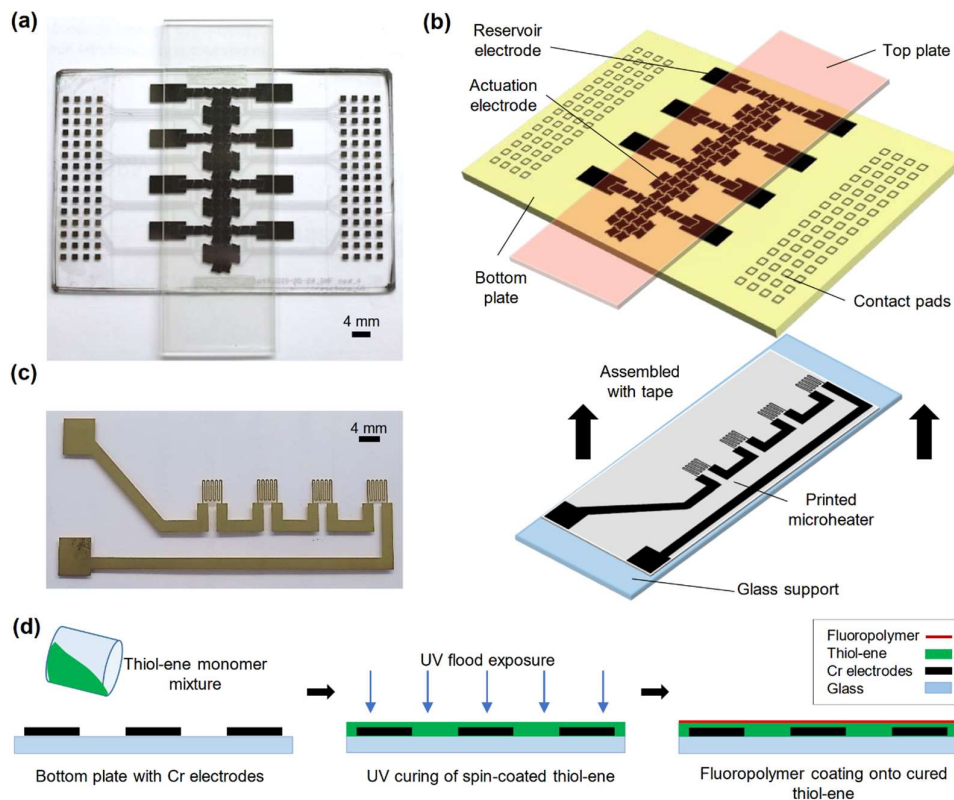

Fig 1. (a) Photograph of a fully assembled DMF device. (b) Schematic illustration of DMF device-microheater assembly. (c) Photograph of a printed microheater array. (d) Protocol for spin coating of thiol-ene (dielectric) and fluoropolymer layers on the DMF bottom plate.

The microheater design, developed for creating physiological temperature on chip, featured four meandering patterns of 200 μm wide lines, each of which covered an area equivalent to four driving electrodes (4 mm × 4 mm) and were interconnected via square contact pads to the power supply (Fig 1c). The microheater patterns were printed with Metalon JS-B25P silver nanoparticle ink onto Novele IJ-220 substrate (NovaCentix, Austin, TX) using an Epson C88+ inkjet printer (Seiko Epson Corporation, Suwa, Japan). After printing, the substrate was heated on a hot plate at 150 °C for 2 min, and the microheater was assembled onto a supporting glass slide and affixed to the bottom of the DMF device using double-sided tape (Fig 1b). For determination of suitable heating power (for enzyme reactions at physiological conditions), the droplet temperature was measured, as described previously,[28] by inserting a miniature thermocouple (wire diameter 50 μm, CHAL-002, OMEGA Engineering, Manchester, UK) in a water droplet of ca. 3 μL embedded between the top and bottom plates. The temperature was recorded with a Fluke 289 multimeter (Fluke Corp., Everett, WA).

Cytochrome P450 activity determination

The magnetic beads incorporating immobilized b-HLM (ca. 0.6 million beads/μL) and the mixture of the pre-fluorescent, enzyme-specific substrate (varies, Table 1) and the cosubstrate (1 mM NADPH) were introduced to the DMF chip by pipetting ca. 6 μL aliquots on to the reservoir electrodes (Fig 1b), after which ca. 1.5 μL aliquots (equivalent to 2-electrode area) of both reagents were dispensed into the DMF device and mixed by electrowetting. The total incubation volume was thus ca. 3 μL (equivalent to 4-electrode area) and the total amount of beads ca. 0.9 million per assay. Theoretically, one batch of 15 million beads thus suffices for as many as 15 technical replicates or alternatively, for 15 parallel analyses of different CYP enzyme activities out of one liver biopsy. In this study, four incubations (technical replicates) were conducted in parallel on a single DMF chip. To reduce biofouling on the DMF chip, 0.1% Pluronic F68 was used as the surfactant in the on-chip enzyme incubations, because the anti-biofouling properties of Pluronics[32] as well as their impact on CYP activity[33] are well-established in the previous literature. The reaction was initiated by applying a heating power of 0.2 W (equal to ca. 37 °C droplet temperature) to the four-in-one microheater, and continued for 30 min under constant mixing of the droplet with the help of DMF actuation (see Supplementary video). The volume loss due to evaporation was compensated by adding ca. 1.5 μL droplet of fresh buffer (equal to a 2-electrode area) to the incubation mixture during incubation based on the evaporation kinetics determined in [28]. The reaction was terminated by switching off the
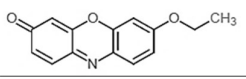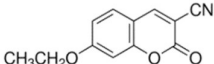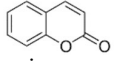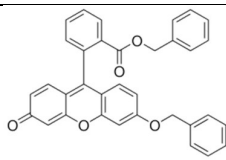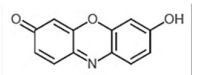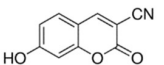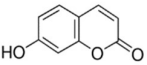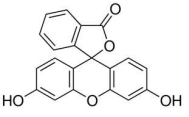
microheater and separating the beads from the reaction solution with the help of a neodymium magnet.

Throughout the experiments, the droplets were actuated using an open-source DropBot automation system[34] by applying 100–120 V_{rms} (at 10 kHz) to the DMF electrodes. The fluorescence originating from the metabolites (Table 1) was analyzed *in situ* by interfacing the chip with a standard well-plate reader (Varioskan LUX, ThermoFisher Scientific, Waltham, MA) upside down and quantitating the fluorescence signal through the transparent cover plate, using the bottom optics of the well-plate reader.[28] The limits of detection and quantitation were determined similarly by quantifying the fluorescence of metabolite standards *in situ*, in the presence of the respective substrate and the cosubstrate NADPH, from droplets equal to a 4-electrode area (ca. 3 µL).

Control incubations with respect to detection specificity were conducted with b-HLM immobilized on microbeads (15 million beads equivalent to ca. 0.25 mg dry weight and 150 µg microsomal total protein) and incubated in microtubes. In this case, however, the full batch of 15 million beads per reaction were incubated in a considerably larger volume (100 µL) compared with the on-chip incubations (ca. 0.9 million beads in 3 µL) and the microtubes were vortexed intermittently to avoid the sedimentation of the beads during incubation. After the incubation, the reaction was terminated by removing the beads, and the supernatant was analyzed by fluorescence on the well-plate reader.

Control incubations were also conducted with soluble (non-immobilized) HLMs, both individual donor-derived and pooled (n=20 donors), in microtubes using model reactions described in Table 1, in a total volume of 100 µL, with total protein concentration of 0.8 mg/mL (HLM), and NADPH concentration of 1 mM. After adding the quenching reagent, the reaction solution was kept on ice for 20 min, centrifuged at 16000 g for 8 min, and the supernatant was analyzed by the well-plate reader.

Table 1: Incubation conditions used for the CYP probe reactions with immobilized and nonimmobilized (control) HLMs. The following abbreviations are used: Ex/em = excitation/emission wavelengths; CEC = 3-cyano-7-ethoxycoumarin; CHC = 3-cyanoumbelliferone; DBF = dibenzylfluorescein; Phosphate = 0.1 M potassium phosphate buffer (pH 7.4) with 5mM $MgCl_2$; Tris = 0.1 M Tris buffer (pH 7.4); NaOH = sodium hydroxide; $HClO_4$ = perchloric acid; ACN = acetonitrile.

Enzymes	CYP1A1/2	CYP1A1/2	CYP2A6	CYP3A4
Substrate (concentration in the activity determination)	7-ethoxyresorufin (2 µM)	CEC (4 µM)	Coumarin (30 µM)	DBF (4 µM)
Metabolite	Resorufin	CHC	Umbelliferone	Fluorescein
Reactions with soluble HLM (0.8 mg/mL)				
Buffer	Phosphate	Tris	Tris	Tris
Time (min)	30	20	20	20
Quenching	2 M NaOH (+10 vol-%)	ACN:Trizma (0.5M) 80:20 (+40 vol-%)	4 M $HClO_4$ (+10 vol-%)	2 M NaOH (+10 vol-%)
Ex/em (nm)	570/590	413/454	325/477	496/516
Reactions with immobilized HLM (both on- and off-chip)				
Buffer	Phosphate	Tris	Tris	Tris
Time (min)	30	30	30	30
Ex/em (nm)	570/590	410/453	331/460	495/516

3. RESULTS AND DISCUSSION

Assay and chip design considerations

Previously, we have preliminarily demonstrated the feasibility of DMF for drug metabolism research in a droplet-scale by using human recombinant CYPs immobilized on porous polymer monoliths affixed onto the DMF platform.[28,29] In this study, we developed a new DMF-based methodology for direct measurement of individual variation in hepatic CYP function using human-derived liver samples in biopsy-scale. Below, we briefly elaborate the assay design principles that were critical to successful execution of CYP activity determination on DMF chips.

In the present work, the method development and validation was conducted using magnetic beads as solid support for HLM immobilization. This was critical to enable handling of ultimately small, biopsy-scale amounts of HLM in a precise manner (Fig 2a–b) by allowing better control over the total surface area compared with the previously employed porous polymer monoliths. According to the developed protocol, the estimated microsomal total protein amount equivalent to that acquired from one liver biopsy (i.e., 250 μg, calculation given in Materials and Methods) yielded 15 million beads, which suffices for ca. 15 on-chip incubations. With average consumption of ca. 0.9 million beads/assay, the calculated amount of microsomal protein consumed (for functionalization of beads) was thereby ca. 15 μg per 0.9 million beads per assay. Thus, the assay design was concluded technically feasible for analysis of biopsy-scale samples. The handling of magnetic beads by DMF can also be automated and is generally well-established in the literature, for example, in the context of immunoprecipitation assays.[35,36] By mixing the reaction solution along a circular path, as illustrated in Fig 2c, precipitation of the beads could also be avoided so as to allow non-restricted mass transfer to and from the enzyme better than that achieved in scaffold-based systems, such as porous polymer monoliths. With a view to kinetic experiments, biotinylation of HLM with the help of fusogenic liposomes is known to preserve the kinetic constants of the critical CYPs similar to those of natural enzymes.[30] A magnetic bead based enzyme reaction can also be terminated accurately by simply separating the beads and extracting the reaction solution for further analysis with the help of DMF actuation. In this manner, theoretically, the beads can also be retrieved for subsequent incubations without denaturing the enzymes, although the re-use possibility was not specifically addressed in this study.
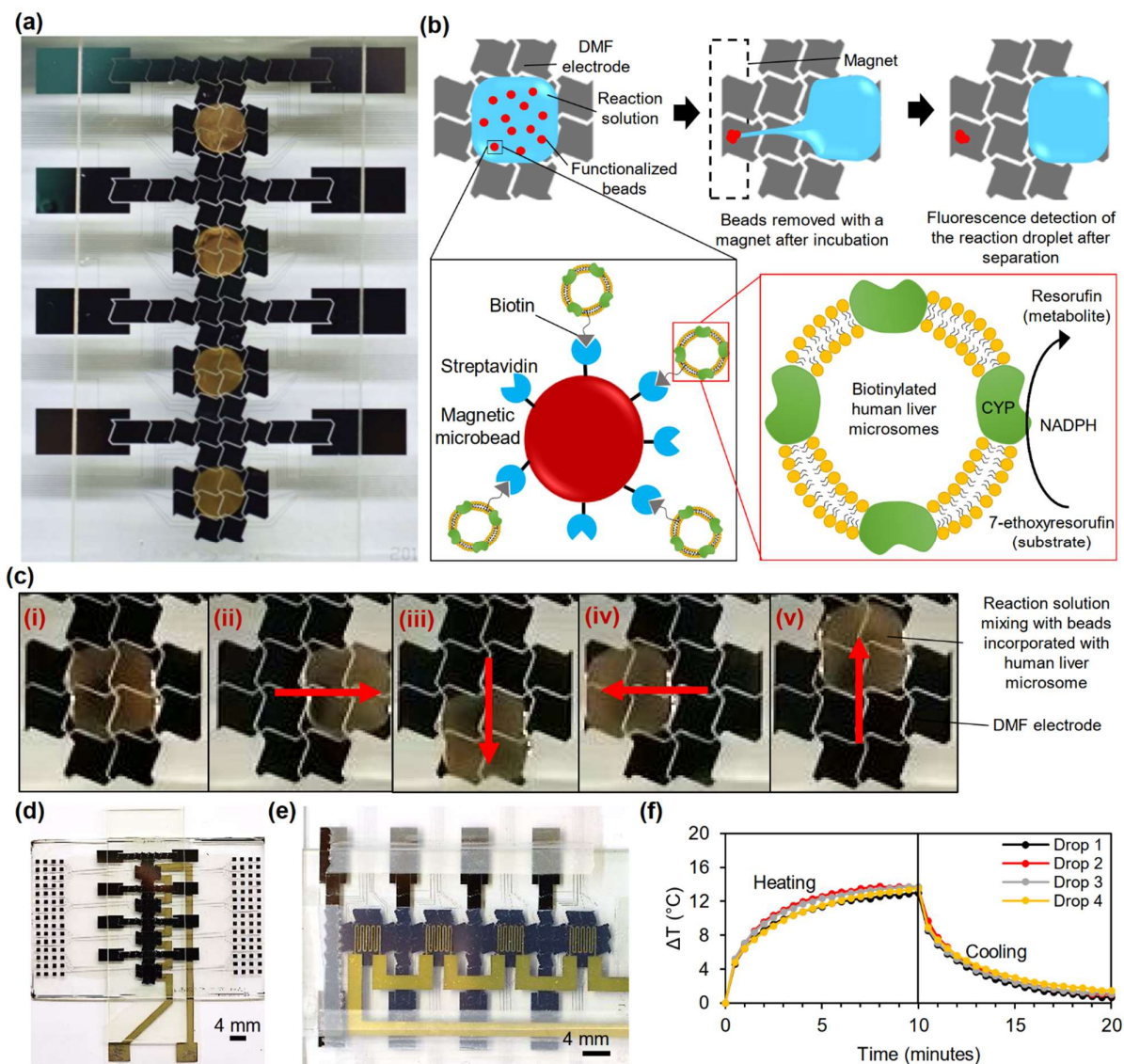
Fig 2. The assay design. (a) Photograph of the DMF device with four reaction droplets containing functionalized beads. (b) Schematic illustration of bead separation protocol of single reaction droplet on DMF device. Insets: Schematic views of CYP immobilization on bead and biotinylated HLM with EROD model reaction. (c) Photographs of the mixing sequence of reaction droplet during CYP incubation on DMF device. (d–e) Photographs of the DMF device-microheater assembly: (d) Top-view and (e) Zoomed-in view from the bottom. (f) Heating and cooling cycles of four sample droplets at four reaction zones at 0.2 W heating power.

Another critical aspect in terms of miniaturization of the hepatic enzyme assays is the narrow temperature range, close to physiological 37 °C, required to ensure that the CYPs preserve their natural clearance kinetics. To address this requirement, we designed a four-in-one microheater element (Figs 2d and e) to enable simultaneous heating of four parallelly performed on-chip enzyme incubations. The microheater design comprised of four 200-µm-wide meandering heater patterns

interconnected with each other and the contact pads via 2-mm-wide lines, ensuring high resistance and local heating only at the meandering parts. The microheater pattern was inkjet-printed on a polymer substrate, which was then affixed below the bottom plate of the DMF device (Figs 2d and e). The heating power required for heating four parallel droplets (each equal to ca. 3 μL) from room temperature (ca. 25 °C) to physiological temperature (ca. 37 °C) was experimentally determined to be ca. 0.2 W. Under these conditions, the heating and cooling curves (Fig 2f), and the temperature stability were well-repeatable between parallel droplets. The temperature variation in individual droplet was within 0.6–3.1% RSD of the mean (n=10 data points over 10 min period).

Method development and selection of the model reaction

The substrate-specificity associated with CYPs (i.e., only one enzyme responsible of drug elimination) is one of critical factors underlying the inter-individual differences in drug response, if the drug's clearance rate is directly proportional to up- and down-regulation of a single CYP form.[3] Besides therapeutic drugs themselves, a plethora of enzyme-specific derivatives of common fluorophores, such as coumarin, fluorescein, and resorufin, have been developed for the assessment of CYP enzyme activities.[37,38] These derivatives are typically low or non-fluorescent themselves, but yield the respective fluorophore as the metabolite via enzyme-specific dealkylation reactions. The resulting coumarin-based metabolites typically fluoresce at the near UV (excitation at ca. 330 nm) or low-end visible (excitation ca. 410 nm) wavelengths, and their detection is thus relatively prone to background interference by material auto-fluorescence. For example, the commonly used dielectric materials in DMF, parylene-C and SU-8 both induce strong auto-fluorescence by short-wavelength excitation.[39,40] In this study, a low-fluorescent thiol-ene polymer was used as a novel dielectric layer material, as it has good optical transmission down to ca. 300 nm.[41] Compared with SU-8, the most commonly used spin-coatable dielectric layer, the thiol-ene layer induced considerably lower auto-fluorescence in the short wavelength range (Fig 3a). At the visible wavelengths equivalent to fluorescein (excitation 495 nm) and resorufin (excitation 570 nm) absorption maxima, the material-induced background was much lower for both materials.
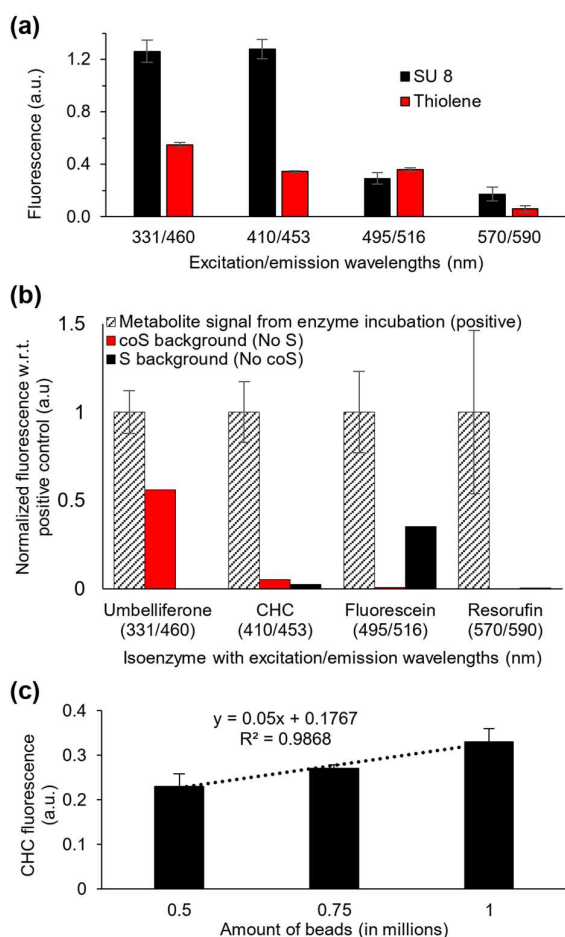
Fig 3. (a) Auto-fluorescence of thiol-ene- and SU-8-coated DMF devices. The error bars represent the standard deviation of n=3 spots per measurement. (b) Selectivity of the metabolite quantitation for the tested model reactions, against with the cosubstrate (coS, 1 mM NADPH) and substrate (S, varies) background from blank control incubations at corresponding wavelengths, when the reactions were conducted with immobilized enzymes off-chip: umbelliferone (CYP2A6), CHC (CYP1A1/2), fluorescein (CYP3A4), and resorufin (CYP1A1/2). The error bars represent the standard deviation from n=3 repeated assays for resorufin and n=4 repeated assays for the others. (c) Effect of total bead count per reaction on the 3-cyano-7-ethoxycoumarin deethylation (CYP1A1/2) activity in on-chip incubations with pooled HLM. The error bars represent the standard deviation of n=3 parallel on-chip assays.

Besides the material-induced background, the detection specificity of the common fluorophores was examined with respect to biological and chemical background arising from the excess pre-fluorescent substrates or the cosubstrate NADPH. This was to ensure that the CYP activity can be flawlessly quantitated by fluorescence *in situ* on the DMF chip, without the need for additional sample preparation steps, such as separation of the soluble reaction components off-chip. For this purpose, the following model reactions yielding two different coumarin derivatives, fluorescein, or resorufin as the metabolite were used: coumarin 7-hydroxylation to umbelliferone (ex 331 nm) via CYP2A6, CEC deethylation to 3-cyanoumbelliferone (ex 410 nm) via CYP1A1 (also to a minor extent via CYP1A2), dibenzylfluorescein dealkylation to fluorescein (ex 495 nm) via CYP3A4, and

ethoxyresorufin O-dealkylation to resorufin (ex 570 nm) via CYP1A1 (also to a minor extent via CYP1A2). The limits of detection of the metabolite standards on the DMF chip for umbelliferone, CHC, fluorescein, and resorufin were 1.0, 0.26, 0.04, and 0.08 pmol, respectively. To determine the specificity of metabolite detection in the incubation matrix, negative control incubations were conducted in the absence of the cosubstrate (equivalent to substrate background) or of the substrate (equivalent to cosubstrate background) and compared with the fluorescence signals obtained from positive control incubations. As a result, the model reactions targeting CYP1A1/2 metabolism, i.e., CEC deethylation (CECOD, ex 410 nm) and ethoxyresorufin O-deethylation (EROD, ex 570 nm), were shown to be reasonably specific in terms of metabolite detection with no background interference arising from the substrate or the cosubstrate (Fig 3b). Thus, these two model reactions were considered suitable for diagnostic CYP activity determination on DMF chips based on *in situ* optical readout by fluorescence. Instead, it was observed that the cosubstrate NAPDH produced substantial optical background in the lowest wavelength tested (ex/em 331/460 nm, equivalent to umbelliferone), which may prevent the use of model reactions yielding umbelliferone as the metabolite unless the reaction components are separated prior to metabolite quantitation (Fig 3b). Similarly, the background signal arising from the chosen fluorescein derivative (dibenzylfluorescein) as a CYP substrate was shown to be significantly high, suggesting that the use of model reactions yielding fluorescein may be prone to quantitation errors due to background interference arising from the substrate or its nonenzymatic degradation products (unless chemically or physically separated from the respective metabolite).

Next, the correlation between the bead count (per reaction) and the metabolic activity was established to ensure that the reaction kinetics was not saturated with respect to the enzyme amount so as to operate under Michaelis-Menten steady state assumption. The preliminary optimization of the bead count (i.e., the amount of immobilized enzyme) per assay was performed with the help of the CECOD reaction (CYP1A1/2). According to CECOD reaction, a linear increase in the metabolite formation was obtained, and thus Michaelis-Menten assumption holds, up to at least one million beads per reaction (Fig 3c). With 0.9 million beads per assay, according to the developed protocol, the apparent hepatic clearance of CECOD reaction (n=3 repeated assays), determined on chip with pooled HLM from 20 donors, was 1.0±0.7 fmol/min.

Method validation

With a view to the precision medicine needs (i.e., personalization of drug dosing on the basis of CYP function), the DMF-based diagnostic protocol was validated by targeting the individual variation in CYP1A1 enzyme activity in five donor samples. Although the CYP1A subfamily has a critical role in, for instance, cancer care and procarcinogen activation, the clinical focus has so far been primarily on CYP1A2. Instead, the importance of the inter-individual variability in CYP1A1 expression to drug pharmacokinetics (metabolism) has only just recently been known.[42]

With a view to the diagnostic possibilities addressing individual variation in CYP1A1 activity, both CECOD and EROD are fairly specific model reactions for CYP1A1 activity (and catalyzed only to a negligible extent by the CYP1A2).[43] However, the EROD reaction was considered a better fit for the diagnostic purposes based on its better detection specificity (Fig 3b) and considerably higher sensitivity with respect to metabolite quantification *in situ* (limit of detection 0.08 pmol EROD vs. 0.26 pmol CECOD). Under optimized conditions (0.9 million beads per assay), the apparent hepatic clearance of EROD reaction (n=5 repeated assays) in pooled HLM was 6.8±1.2 fmol/min.

The individual variation in EROD activities was first determined by control incubations off-chip and compared with that of phenacetin O-deethylation activity (a considerably specific marker of CYP1A2) reported by the supplier of the donor HLMs (Fig 4a). As a result, substantial differences in the relative activities of EROD (primarily via CYP1A1) and phenacetin O-deethylation (primarily via CYP1A2) were observed between individuals, confirming the fact that the CYP1A1 activity cannot be directly predicted on the basis of CYP1A2 activity. Unlike CYP1A2 activity (typically traced *in vivo* via phenacetin administration[44]), CYP1A1 activity determination *in vivo* lacks standardized pharmacokinetic markers that could be dosed to patients, which justifies the usefulness of the DMF-based diagnostic test, designated for CYP1A1, in the assessment of the individual variability in this enzyme function.

With a view to biopsy-scale analysis of EROD activity, the specificity of the DMF-based assay was further confirmed with the help of five positive controls (0.9 million beads per reaction) and three negative controls (in the absence of substrate, cosubstrate, or both) using beads functionalized with pooled HLM. A significant difference ($p = 0.026$, two-tailed t-test) was obtained between the average fluorescence signals from positive (0.5±0.1 a.u.) and negative (0.2±0.1 a.u.) controls. The inter-assay repeatability was also good (18.3% RSD, n=5 assays), which provided solid basis for determination of the individual EROD activities of the donor samples. The experimental variation between technical replicates was also used as a measure to evaluate whether the DMF assay is capable of revealing the

biological variation in the EROD activities between individuals. Next, the EROD activities were determined for five individuals (Donors A–E, n=4 repeated DMF assays per each individual), which manifested substantial variation between donors (Fig 4b). In two cases out of five the difference of individual EROD activity to that of the pool of 20 donors was statistically significant (Fig 4b), suggesting that the variation is of biological origin. However, it should be noted that the pool only represents an artificial population average tailor-made for preclinical drug discovery purposes and as such, it is not a suitable measure for categorizing patients between extensive and poor metabolizers. But in this study, comparison of individual samples against the pool provided a solid measure for assessment of the technical feasibility of the developed protocol for distinguishing patient samples between low and high metabolic (EROD) capacity.
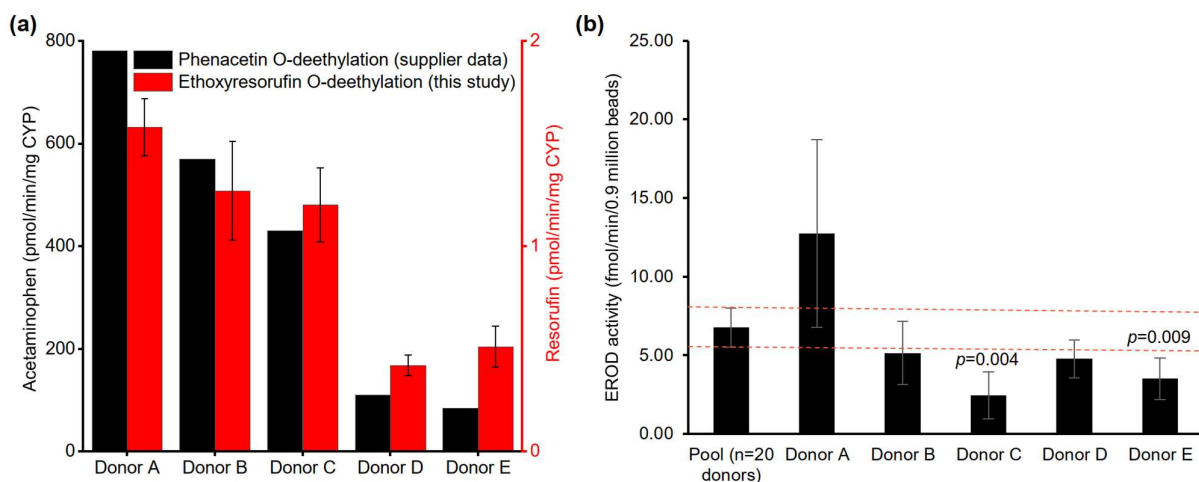

Fig 4. (a) Comparison of the clearance rates of phenacetin (supplier data) and ethoxyresorufin (in-house data derived from control incubations with soluble, non-immobilized enzymes) in pooled (n=20) and individual donor HLM. (b) EROD activity of pooled (n=20) and individual donor HLMs. The error bars represent the standard deviation of n=4 repeated assays in each case in (a) and (b), and *p* values in (b) were calculated using two-tailed t-test.

CONCLUSIONS

In this study, we conceptualized magnetic bead based, DMF-enabled CYP enzyme activity assays in biopsy scale and demonstrated their technical feasibility for determining up-/down-regulation of hepatic EROD activities between individuals. The chip design used in this study incorporated electrical actuators both for sample handling (DMF) and for maintaining physiological temperature on chip (an integrated, inkjet-printed microheater array). This enabled performing four simultaneous CYP activity analyses in an automated manner in a parallelized system. As the amount of microsomal protein consumed for functionalizing sufficient number of beads was only about 15 μg per assay, the developed protocol is readily technically feasible for determination of a patient's hepatic CYP

activities, for instance, in the context of other biopsy-based liver disease diagnoses to support personalization of CYP-mediated medical therapies. Supported by the constantly increasing technology readiness level and automation of DMF, the developed protocol is foreseen as the first step forward toward the development of highly automated clinical diagnostics for precision medicine (from the perspective of drug dosing). However, the feasibility of the assay for clinical use is also largely dependent on the quality of biopsy-taking, which may affect the enzyme function, as well as the use of appropriate *in vitro-in vivo* scaling factors, as usual.

Supplementary material: Video V1 of the bead incubation.

ACKNOWLEDGEMENTS

REFERENCES

(1)   Zanger, U. M.; Turpeinen, M.; Klein, K.; Schwab, M. Functional Pharmacogenetics/Genomics of Human Cytochromes P450 Involved in Drug Biotransformation. *Anal Bioanal Chem* **2008**, *392* (6), 1093–1108. https://doi.org/10.1007/s00216-008-2291-6.

(2)   Nebert, D. W.; Russell, D. W. Clinical Importance of the Cytochromes P450. *The Lancet* **2002**, *360* (9340), 1155–1162. https://doi.org/10.1016/S0140-6736(02)11203-7.

(3)   Zanger, U. M.; Schwab, M. Cytochrome P450 Enzymes in Drug Metabolism: Regulation of Gene Expression, Enzyme Activities, and Impact of Genetic Variation. *Pharmacology & Therapeutics* **2013**, *138* (1), 103–141. https://doi.org/10.1016/j.pharmthera.2012.12.007.

(4)   Androutsopoulos, V. P.; Tsatsakis, A. M.; Spandidos, D. A. Cytochrome P450 CYP1A1: Wider Roles in Cancer Progression and Prevention. *BMC Cancer* **2009**, *9* (1), 187. https://doi.org/10.1186/1471-2407-9-187.

(5)   Schiwy, A.; Brinkmann, M.; Thiem, I.; Guder, G.; Winkens, K.; Eichbaum, K.; Nüßer, L.; Thalmann, B.; Buchinger, S.; Reifferscheid, G.; Seiler, T.-B.; Thoms, B.; Hollert, H. Determination of the CYP1A-Inducing Potential of Single Substances, Mixtures and Extracts of Samples in the Micro-EROD Assay with H4IIE Cells. *Nat. Protocols* **2015**, *10* (11), 1728–1741. https://doi.org/10.1038/nprot.2015.108.

(6)   Anwar-Mohamed, A.; Elbekai, R. H.; El-Kadi, A. O. Regulation of CYP1A1 by Heavy Metals and Consequences for Drug Metabolism. *Expert Opin Drug Metab Toxicol* **2009**, *5* (5), 501–521. https://doi.org/10.1517/17425250902918302.

(7)   Abass, K.; Pelkonen, O. The Inhibition of Major Human Hepatic Cytochrome P450 Enzymes by 18 Pesticides: Comparison of the N-in-One and Single Substrate Approaches. *Toxicol In Vitro* **2013**, *27* (5), 1584–1588. https://doi.org/10.1016/j.tiv.2012.05.003.

(8)   Franz, C. C.; Egger, S.; Born, C.; Rätz Bravo, A. E.; Krähenbühl, S. Potential Drug-Drug Interactions and Adverse Drug Reactions in Patients with Liver Cirrhosis. *Eur. J. Clin. Pharmacol.* **2012**, *68* (2), 179–188. https://doi.org/10.1007/s00228-011-1105-5.

(9)   Frye, R. F.; Zgheib, N. K.; Matzke, G. R.; Chaves-Gnecco, D.; Rabinovitz, M.; Shaikh, O. S.; Branch, R. A. Liver Disease Selectively Modulates Cytochrome P450--Mediated Metabolism. *Clin. Pharmacol. Ther.* **2006**, *80* (3), 235–245. https://doi.org/10.1016/j.clpt.2006.05.006.

(10)   Moaddeb, J.; Haga, S. B. Pharmacogenetic Testing: Current Evidence of Clinical Utility. *Ther Adv Drug Saf* **2013**, *4* (4), 155–169. https://doi.org/10.1177/2042098613485595.

(11)   Maciel, A.; Cullors, A.; Lukowiak, A. A.; Garces, J. Estimating Cost Savings of Pharmacogenetic Testing for Depression in Real-World Clinical Settings. *Neuropsychiatr Dis Treat* **2018**, *14*, 225–230. https://doi.org/10.2147/NDT.S145046.

(12)   Zhang, C.; Shi, L.; Wang, F.-S. Liver Injury in COVID-19: Management and Challenges. *The Lancet Gastroenterology & Hepatology* **2020**, *5* (5), 428–430. https://doi.org/10.1016/S2468-1253(20)30057-1.

(13)   Tanaka, E. Clinical Importance of Non-Genetic and Genetic Cytochrome P450 Function Tests in Liver Disease. *Journal of Clinical Pharmacy and Therapeutics* **1998**, *23* (3), 161–170. https://doi.org/10.1046/j.1365-2710.1998.00135.x.

(14)   Fujiki, Y.; Hubbard, A. L.; Fowler, S.; Lazarow, P. B. Isolation of Intracellular Membranes by Means of Sodium Carbonate Treatment: Application to Endoplasmic Reticulum. *J. Cell Biol.* **1982**, *93* (1), 97–102. https://doi.org/10.1083/jcb.93.1.97.

(15)   Ekins, S.; Ring, B. J.; Grace, J.; McRobie-Belle, D. J.; Wrighton, S. A. Present and Future in Vitro Approaches for Drug Metabolism. *Journal of Pharmacological and Toxicological Methods* **2000**, *44* (1), 313–324. https://doi.org/10.1016/S1056-8719(00)00110-6.

(16)   Bodero, M.; Francisco Abisambra, J. Microsome Isolation from Tissue. *Bio Protoc* **2014**, *4* (3).

(17)   Naritomi, Y.; Terashita, S.; Kimura, S.; Suzuki, A.; Kagayama, A.; Sugiyama, Y. Prediction of Human Hepatic Clearance from in Vivo Animal Experiments and in Vitro Metabolic Studies with Liver Microsomes from Animals and Humans. *Drug Metab Dispos* **2001**, *29* (10), 1316–1324.

(18)   Hakooz, N.; Ito, K.; Rawden, H.; Gill, H.; Lemmers, L.; Boobis, A. R.; Edwards, R. J.; Carlile, D. J.; Lake, B. G.; Houston, J. B. Determination of a Human Hepatic Microsomal Scaling Factor for Predicting in Vivo Drug Clearance. *Pharm Res* **2006**, *23* (3), 533–539. https://doi.org/10.1007/s11095-006-9531-2.

(19)   Sato, N.; Kamada, T.; Abe, H.; Suematsu, T.; Kawano, S.; Hayashi, N.; Matsumura, T.; Hagihara, B. Simultaneous Measurement of Mitochondrial and Microsomal Cytochrome Levels in Human Liver Biopsy. *Clin. Chim. Acta* **1977**, *80* (2), 243–251. https://doi.org/10.1016/0009-8981(77)90031-6.

(20)   Zhang, H.; Gao, N.; Tian, X.; Liu, T.; Fang, Y.; Zhou, J.; Wen, Q.; Xu, B.; Qi, B.; Gao, J.; Li, H.; Jia, L.; Qiao, H. Content and Activity of Human Liver Microsomal Protein and Prediction of Individual Hepatic Clearance in Vivo. *Scientific Reports* **2015**, *5* (1), 17671. https://doi.org/10.1038/srep17671.

(21)   Yan, T.; Lu, L.; Xie, C.; Chen, J.; Peng, X.; Zhu, L.; Wang, Y.; Li, Q.; Shi, J.; Zhou, F.; Hu, M.; Liu, Z. Severely Impaired and Dysregulated Cytochrome P450 Expression and Activities in Hepatocellular Carcinoma: Implications for Personalized Treatment in Patients. *Mol Cancer Ther* **2015**, *14* (12), 2874–2886. https://doi.org/10.1158/1535-7163.MCT-15-0274.

(22)   Choi, K.; Ng, A. H. C.; Fobel, R.; Wheeler, A. R. Digital Microfluidics. *Annual Review of Analytical Chemistry* **2012**, *5* (1), 413–440. https://doi.org/10.1146/annurev-anchem-062011-143028.

(23)   Ng, A. H. C.; Fobel, R.; Fobel, C.; Lamanna, J.; Rackus, D. G.; Summers, A.; Dixon, C.; Dryden, M. D. M.; Lam, C.; Ho, M.; Mufti, N. S.; Lee, V.; Asri, M. A. M.; Sykes, E. A.; Chamberlain, M. D.; Joseph, R.; Ope, M.; Scobie, H. M.; Knipes, A.; Rota, P. A.; Marano, N.; Chege, P. M.; Njuguna, M.; Nzunza, R.; Kisangau, N.; Kiogora, J.; Karuingi, M.; Burton, J. W.; Borus, P.; Lam, E.; Wheeler, A. R. A Digital Microfluidic System for Serological Immunoassays in Remote Settings. *Science Translational Medicine* **2018**, *10* (438). https://doi.org/10.1126/scitranslmed.aar6076.

(24)   Yafia, M.; Ahmadi, A.; Hoorfar, M.; Najjaran, H. Ultra-Portable Smartphone Controlled Integrated Digital Microfluidic System in a 3D-Printed Modular Assembly. *Micromachines* **2015**, *6* (9), 1289–1305. https://doi.org/10.3390/mi6091289.

(25)   Millington, D.; Norton, S.; Singh, R.; Sista, R.; Srinivasan, V.; Pamula, V. Digital Microfluidics Comes of Age: High-Throughput Screening to Bedside Diagnostic Testing for Genetic Disorders in Newborns. *Expert Rev Mol Diagn* **2018**, *18* (8), 701–712. https://doi.org/10.1080/14737159.2018.1495076.

(26) Mousa, N. A.; Jebrail, M. J.; Yang, H.; Abdelgawad, M.; Metalnikov, P.; Chen, J.; Wheeler, A. R.; Casper, R. F. Droplet-Scale Estrogen Assays in Breast Tissue, Blood, and Serum. *Science Translational Medicine* **2009**, *1* (1), 1ra2-1ra2. https://doi.org/10.1126/scitranslmed.3000105.

(27) Shih, S. C. C.; Yang, H.; Jebrail, M. J.; Fobel, R.; McIntosh, N.; Al-Dirbashi, O. Y.; Chakraborty, P.; Wheeler, A. R. Dried Blood Spot Analysis by Digital Microfluidics Coupled to Nanoelectrospray Ionization Mass Spectrometry. *Anal. Chem.* **2012**, *84* (8), 3731–3738. https://doi.org/10.1021/ac300305s.

(28) Sathyanarayanan, G.; Haapala, M.; Kiiski, I.; Sikanen, T. Digital Microfluidic Immobilized Cytochrome P450 Reactors with Integrated Inkjet-Printed Microheaters for Droplet-Based Drug Metabolism Research. *Anal Bioanal Chem* **2018**, *410* (25), 6677–6687. https://doi.org/10.1007/s00216-018-1280-7.

(29) Sathyanarayanan, G.; Haapala, M.; Sikanen, T. Interfacing Digital Microfluidics with Ambient Mass Spectrometry Using SU-8 as Dielectric Layer. *Micromachines* **2018**, *9* (12), 649. https://doi.org/10.3390/mi9120649.

(30) Kiiski, I.; Pihlaja, T.; Urvas, L.; Wiedmer, S.; Jokinen, V.; Sikanen, T. Overcoming the Pitfalls of Cytochrome P450 Immobilization Through the Use of Fusogenic Liposomes. *Advanced Biosystems* **2018**, *accepted*. https://doi.org/10.1002/adbi.201800245.

(31) Sathyanarayanan, G.; Haapala, M.; Dixon, C.; Wheeler, A. R.; Sikanen, T. M. A Digital-to-Channel Microfluidic Interface via Inkjet Printing of Silver and UV Curing of Thiol–Enes. *Advanced Materials Technologies* **2020**. https://doi.org/10.1002/admt.202000451.

(32) Luk, V. N.; Mo, G. CH.; Wheeler, A. R. Pluronic Additives: A Solution to Sticky Problems in Digital Microfluidics. *Langmuir* **2008**, *24* (12), 6382–6389. https://doi.org/10.1021/la7039509.

(33) Ollikainen, E.; Liu, D.; Kallio, A.; Mäkilä, E.; Zhang, H.; Salonen, J.; Santos, H. A.; Sikanen, T. M. The Impact of Porous Silicon Nanoparticles on Human Cytochrome P450 Metabolism in Human Liver Microsomes in Vitro. *European Journal of Pharmaceutical Sciences* **2017**, *104*, 124–132. https://doi.org/10.1016/j.ejps.2017.03.039.

(34) Fobel, R.; Fobel, C.; Wheeler, A. R. DropBot: An Open-Source Digital Microfluidic Control System with Precise Control of Electrostatic Driving Force and Instantaneous Drop Velocity Measurement. *Appl. Phys. Lett.* **2013**, *102* (19), 193513. https://doi.org/10.1063/1.4807118.

(35) Coudron, L.; McDonnell, M. B.; Munro, I.; McCluskey, D. K.; Johnston, I. D.; Tan, C. K. L.; Tracey, M. C. Fully Integrated Digital Microfluidics Platform for Automated Immunoassay; A Versatile Tool for Rapid, Specific Detection of a Wide Range of Pathogens. *Biosensors and Bioelectronics* **2019**, *128*, 52–60. https://doi.org/10.1016/j.bios.2018.12.014.

(36) Ng, A. H. C.; Choi, K.; Luoma, R. P.; Robinson, J. M.; Wheeler, A. R. Digital Microfluidic Magnetic Separation for Particle-Based Immunoassays. *Anal. Chem.* **2012**, *84* (20), 8805–8812. https://doi.org/10.1021/ac3020627.

(37) Donato, M. T.; Jiménez, N.; Castell, J. V.; Gómez-Lechón, M. J. Fluorescence-Based Assays for Screening Nine Cytochrome P450 (P450) Activities in Intact Cells Expressing Individual Human P450 Enzymes. *Drug Metab. Dispos.* **2004**, *32* (7), 699–706. https://doi.org/10.1124/dmd.32.7.699.

(38) Stresser, D. M.; Turner, S. D.; Blanchard, A. P.; Miller, V. P.; Crespi, C. L. Cytochrome P450 Fluorometric Substrates: Identification of Isoform-Selective Probes for Rat CYP2D2 and Human CYP3A4. *Drug Metab. Dispos.* **2002**, *30* (7), 845–852. https://doi.org/10.1124/dmd.30.7.845.

(39) Lu, B.; Zheng, S.; Quach, B. Q.; Tai, Y.-C. A Study of the Autofluorescence of Parylene Materials for MicroTAS Applications. *Lab Chip* **2010**, *10* (14), 1826–1834. https://doi.org/10.1039/b924855b.

(40) Walczak, R.; Sniadek, P.; Dziuban, J. A. SU-8 Photoresist as Material of Optical Passive Components Integrated with Analytical Microsystems for Real-Time Polymerase Chain Reaction. *Optica Applicata* **2011**, *Vol. 41* (nr 4).

(41) Feidenhans'l, N. A.; Lafleur, J. P.; Jensen, T. G.; Kutter, J. P. Surface Functionalized Thiol-Ene Waveguides for Fluorescence Biosensing in Microfluidic Devices. *ELECTROPHORESIS* **2014**, *35* (2–3), 282–288. https://doi.org/10.1002/elps.201300271.

(42) Lang, D.; Radtke, M.; Bairlein, M. Highly Variable Expression of CYP1A1 in Human Liver and Impact on Pharmacokinetics of Riociguat and Granisetron in Humans. *Chem. Res. Toxicol.* **2019**, *32* (6), 1115–1122. https://doi.org/10.1021/acs.chemrestox.8b00413.

(43) Zamaratskaia, G.; Zlabek, V. EROD and MROD as Markers of Cytochrome P450 1A Activities in Hepatic Microsomes from Entire and Castrated Male Pigs. *Sensors (Basel)* **2009**, *9* (3), 2134–2147. https://doi.org/10.3390/s90302134.

(44) Pu, X.; Gao, Y.; Li, R.; Li, W.; Tian, Y.; Zhang, Z.; Xu, F. Biomarker Discovery for Cytochrome P450 1A2 Activity Assessment in Rats, Based on Metabolomics. *Metabolites* **2019**, *9* (4). https://doi.org/10.3390/metabo9040077.